Petroleum Research 8 (2023) 256–269

Contents lists available at ScienceDirect

Petroleum Research

journal homepage: http://www.keaipublishing.com/en/journals/petroleum-research/

Performance evaluation of nanosilica derived from agro-waste as lost circulation agent in water-based mud

Augustine Agi [a, *], Jeffrey O. Oseh [b, c, e], Afeez Gbadamosi [d], Cheo Kiew Fung [b, e], Radzuan Junin [b, e], Mohd Zaidi Jaafar [b, e]

[a] Faculty of Chemical and Process Engineering Technology, College of Engineering Technology, Universiti Malaysia Pahang, 26300, Gambang, Pahang, Malaysia
[b] Institute for Oil and Gas (IFOG), Universiti Teknologi Malaysia, 81310, Johor Bahru, Malaysia
[c] Federal University of Technology, P.M.B. 1526, Owerri, Imo State, Nigeria
[d] Department of Petroleum Engineering, College of Petroleum and Geosciences, King Fahd University of Petroleum and Minerals, 31261, Dhahran, Saudi Arabia
[e] Department of Petroleum Engineering, School of Chemical and Energy Engineering, Faculty of Engineering, Universiti Teknologi Malaysia, 81310 Johor Bahru, Malaysia

ARTICLE INFO

Article history:
Received 17 December 2021
Received in revised form
27 July 2022
Accepted 29 July 2022
Available online 4 August 2022

Keywords:
Rice husk silica nanoparticles
Loss circulation material
Fractured formation
Water based-mud
Rheology

ABSTRACT

Seepage or loss of the mix-water from the drilling muds into the porous and permeable formations is a common problem during drilling operation. The drilling mud design requires a good knowledge of sealing integrity and all the factors influencing the mud to bridge through fractures or pore throat of exposed rocks. Loss circulation materials (LCMs) are commonly introduced into the drilling mud to prevent or minimize filtrate loss. This study investigates silica nanoparticle (SNP) derived from rice husk (RH) termed RH-SNP using the wet-milling method as an LCM in water-based mud (WBM). The impact of the RH-SNP in the enhancement of rheology and filtrate loss control properties of WBM was studied. Subsequently, the sealing integrity of the RH-SNP in a 1 mm and 2 mm simulated fracture for 7 min was determined using a stainless-steel slotted filter disk. The performance of the developed RH-SNP was compared with the widely applied nutshell. The synthesized RH-SNP at amount of 2.0 wt% significantly enhanced the yield point and plastic viscosity of the WBM by 75% and 386%, respectively, and minimized the fluid loss of the WBM by 47% at 80 °F. The enhancement is due to the particles ability to spread and interact efficiently with the WBM. With the use of 1 mm and 2 mm simulated fracture for 7 min, the mud loss volume of the base mud reduced by 50%, 66.7%, 86%, and 90% (for 1 mm) and 40%, 65.7%, 77.1%, and 80% (for 2 mm) with the inclusion of 0.5 wt%, 1.0 wt%, 1.5 wt%, and 2.0 wt% of RH-SNP, respectively. Overall, the results showed that RH-SNP enhanced the seal integrity of the drilling mud and was more resistant to deformation compared to the nutshell. The findings of this study can help for better understanding of the application of RH-SNP as a loss circulation agent owing to its superior ability to seal fractured formation compared with the often used nutshell.

1. Introduction

The success of any drilling operation hinges strongly on the compositions and properties of the drilling fluid used (Fadairo et al., 2021). Drilling muds are introduced to drill oil wells, natural gas wells, exploratory drilling rigs, and water wells, such as boreholes. These drilling muds are utilized to lift drilled cuttings to the surface from the bottom of the wellbore and to suspend drilled cuttings from sedimentation during stoppage (Davarpanah, 2018; Saleh and Ibrahim, 2021). They are also used to cool and lubricate drill bits and pipes, control formation pressure, encapsulate and inhibit shale swelling, stabilize rocks and drilled wellbore (Rafati et al., 2018; Smith et al., 2018; Broni-Bediako and Amorin, 2019). The cooling and lubrication contribute to extend the life of the drill bit.

* Corresponding author. Faculty of Chemical and Process Engineering Technology, College of Engineering Technology, Universiti Malaysia Pahang, 26300, Gambang, Pahang, Malaysia
E-mail address: augustine@ump.edu.my (A. Agi).

https://doi.org/10.1016/j.ptlrs.2022.07.005

Overtime, loss of drilling fluid (lost circulation) is one of the most severe problems encountered in the process of drilling. Lost circulation occurs when drilling mud (or fluid) incessantly flows into the formation being drilled or fails to return to the surface after being pumped downhole (Mahto and Jain, 2013). Huge volumes of fluid can be lost before a proper filter cake forms, or the loss can carry on for an unlimited period. Lost circulation is also encountered when the drill bit bump into caverns, fractures or natural fissures, and mud flows into the newly available space. The application of higher mud pressure than the formation can withstand (i.e., overbalanced drilling) can open the fracture into which the mud flows (Yildirim et al., 2016; Khalifeh et al., 2019). When lost circulation take place, sealing the zone is indispensable unless the geological environments permit blind drilling, which is unlikely in most cases (Khalifeh et al., 2019). To address this problem, prevention is critical, but, due to the reason that lost circulation is a common incidence, effective ways and means of treatment are also a high priority.

Conventional and relatively low-cost materials often used for lost circulation treatments include paper, sized calcium carbonate, nutshells, cellophane, mica, and cotton seed hulls (Salehi and Nygaard, 2012). These materials are available in fine, medium, and coarse grades and are typically mixed with the drilling mud to seal loss productive zones; they can also be grouped as flaked, fibrous, granular, a combination of flaked, fibrous, and granular materials (Salehi and Nygaard, 2012; Yildirim et al., 2016). However, these conventional and low-cost LCMs have some flaws. The main flaws are their poor thermal stability, hydration tendency when they are mixed with water, premature gelation, and difficulty in spotting them at the right location (Wang et al., 2012). Also, they are easily extruded into the formation and are found to be less environmentally benign (Lecolier et al., 2005; Ismail et al., 2020).

Researchers have sought different ways to combat these problems and more recently nanotechnology (Alwated and El-Amin, 2021; Panchal et al., 2021; Ahasan et al., 2022). Nanotechnology has found usefulness in the oil and gas industry and has been recommended as one of the ways to treat lost circulation (Ali et al., 2020; Saleh, 2022). The application of nanotechnology for drilling fluids has exhibited favourable results in mitigating fluid loss problems, bridging of pores and fractures, and treating lost circulation (Gbadamosi et al., 2019a; Ali et al., 2020; Oseh et al., 2020a, 2020b; Blkoor et al., 2021). Oseh et al. (2020a) demonstrated that SiO_2 NPs can decrease the filtrate loss volume and friction coefficient of complex drilling muds. The findings of other studies conducted with SiO_2 NPs showed improvement in drilling fluid rheological properties (Smith et al., 2018; Boyou et al., 2019; Gbadamosi et al., 2019b; Blkoor et al., 2022), enhancement in wellbore cleaning, and cutting transport process (Agi et al., 2019a, 2019b; Gbadamosi et al., 2019a; Oseh et al., 2020b). SiO_2 NPs are also found to increase the yield point (YP) of conventional water-based mud (WBM) and are stable at high pressure and high temperature (HPHT) environments (Oseh et al., 2020c). Furthermore, they contributed to the improvement of the shale inhibiting property of the WBM and inhibition of clay dispersion (Xuan et al., 2014; Medhi et al., 2020; Oseh et al., 2020c; Saleh, 2022).

To mitigate fluid loss Anawe et al. (2004) evaluated the use of RH in oil-based mud. The potential of the RH to minimize lost circulation was compared with that of sawdust. The study observed that RH yielded higher values of mud density and viscosities, whereas the sawdust-based mud produced lower values of viscosities and mud density. In the same vein, Okon et al. (2014) evaluated RH potential to minimize filtrate loss of a WBM and compared its efficiency with carboxyl methyl cellulose (CMC) and polyanionic cellulose-reagent grade (PAC-R). They reported that RH produced desirable filtrate loss control close to the two-modified cellulose natural polymers. The authors concluded that RH is an efficient filtrate loss control agent but could require some additional manipulations to have more desirable filter cakes. Moreover, these studies did not account for treatment of lost circulation through bridging materials, especially with nanosized range particles. Thus, it was deemed important in this study to understand the pore scale and fractures sealing characteristics of rice husk ash silica NP (RH-SNP) in conventional WBM system using a bridging material test on simulated fracture disk. RH can provide good compressive strength to the drilling mud. It is an agro by-product; thus, it contributes to cutting down the environmental pollution. The high SiO_2 content makes it a good supplement for drilling fluid (Wang et al., 2012). RH when burnt in the boiler as fuel, produces ash known as rice husk ash (RHA). The environmental waste RHA contains about 80–90% SiO_2 in amorphous form, and is lightweight, highly porous structure, with high specific surface area, and is very valuable in various industries (Wang et al., 2012).

Therefore, this research proposes the use of locally derived, cost-effective agro by-product, and eco-friendly RH-SNP in complex WBM system for fluid loss control and treatment of lost circulation, thereby fostering a circular economy. The research goal was achieved by evaluating the ability of the RH-SNP to impact rheological and filtrate loss control properties of the WBM. It was followed by examining the seal integrity and performance of the locally derived RH-SNP in a simulated fractured formation to mimic a fractured production zone. This investigation was compared with the widely applied industrial nutshell to understand the performance and potentials of the eco-friendly RH-SNP for lost circulation treatment.

2. Materials and methods

2.1. Materials

The RH used in this research was obtained from a local rice mill in Johor, Malaysia. Analytical reagent grade hydrochloride acid (HCl of 37 wt%), molecular biological grade ethanol with purity 96%, distilled water, and deionized water were purchased from Merck Group (Sdn. Bhd., Selangor, Malaysia). Calcium chloride ($CaCl_2$) (Molecular weight of 110.98 g/mol, purity of 97%), nonionic polyanionic cellulose (PAC), caustic soda (NaOH), and soda ash (Na_2CO_3) were obtained from Sigma-Aldrich. Sodium bentonite, nutshell, and barite were purchased from Scomi Oiltools, Malaysia. The chemicals were used as acquired without any purification except the RH that was processed into RH-SNP.

2.2. Methods

A summarized plan of the study process containing the experimental works is presented in Fig. 1.

2.2.1. Synthesis of RH-SNP

The preparation of RH-SNP was achieved by wet milling process. The RH was washed with water for several times to remove dirt and other contaminants. It was then dried at 80 °C for 12 h. Thereafter, the dried RH was burnt using a Thermolyne 30400 Laboratory Furnace, Barnstead, USA and heated at 400 °C for 2 h and then kept at 700 °C for 2 h. At 400 °C, the organic constituents disintegrated and at 700 °C, large amount of ash with high content of SiO_2 was obtained. At 700 °C, the amount of carbonaceous material (lignin and cellulose) present in the RH was decreased and more SiO_2 content was recovered. The obtained white RHA was used to extract the SiO_2 and prepare the RH-SNP. 30 g of the RHA sample was added to 50 wt% HCl solution and stirred for 2 h, to remove the metal ions. Although the organic constituents were removed by thermal breakdown at 400 °C, metal cations, like K^+, can catalyze

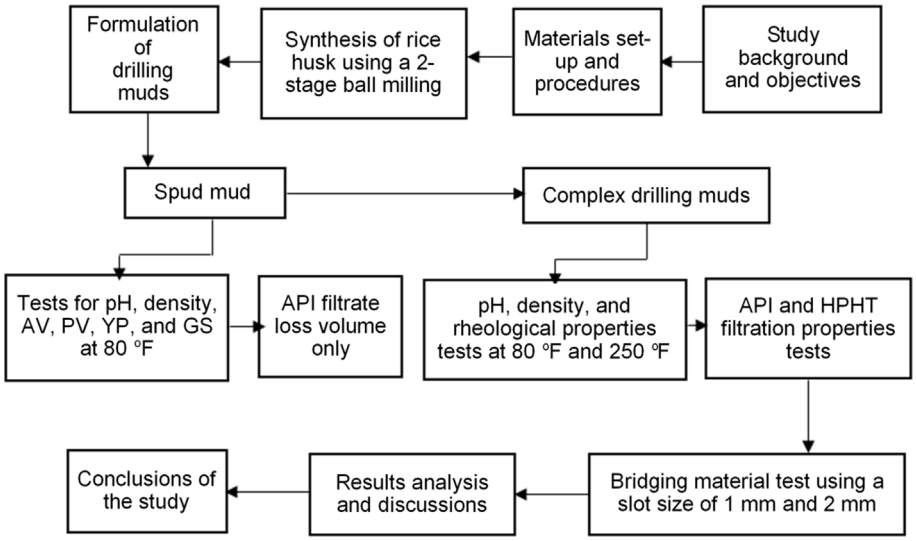

Fig. 1. The study flow plan.

the melting of SiO_2 if not removed (Wang et al., 2012). The resulting white powder was filtered and washed several times with distilled water until the pH value equals 7 (neutral). The washed RH powder was dried at 80 °C for 3 h under vacuum.

Afterwards, a two-stage ball milling process was used to reduce the particles to nanosize. By decreasing the RH particle size to the nanometer scale (RH-SNP), the energy gap of the electronic structure is transformed to discrete electronic states with many atoms emerging on the surface (Saleh and Ibrahim, 2021). Thus, these large number of atoms will become more energetic due to the growing distance between the atomic structures and the unsaturated sites. A planetary ball mill machine DECO121 PBM-V-2L-A; DECO, China containing a 250 ml tungsten carbide grinding jar was loaded with 150 ml of tungsten carbide balls and 85 ml of RH. It was milled for 2 h at 400 rpm; this was done to achieve homogenous particle sizes (Zhang et al. 2013, 2017). The sample was then dispersed in ethanol, which acted in place of surfactant as micelle maker to prevent agglomeration of the particles and control the size of the RH-SNP. Then, wet milling of the sample was performed for 5 h at 400 rpm to achieve nanosize. The sample was collected and dried in an oven at 80 °C for 17 h.

2.2.2. Preparation of drilling muds

2.2.2.1. Spud mud formulation. Before using additives to formulate drilling muds for drilling a well, such additives need to meet some basic conditions, such as desirable thermal stability, improved rheology and filtration properties, ability to inhibit shale effectively, and lubricate the drilling apparatus. To this effect, two categories of WBMs were formulated: spud muds and complex drilling muds. An unweighted spud mud was prepared first and tested. Later, complex WBM systems were prepared. Spud muds are usually used to drill the surface hole. Usually, an onshore spud mud contains bentonite flocculated with lime, water as the base liquid, and NaOH (Singh and Dutta, 2018). On this basis, spud mud was formulated according to 1 lab. barrel = 350 ml in the following manner:

Spud mud (base mud) = 350 ml tap water + 20 wt% sodium bentonite + 2.0 wt% NaOH. Thereafter, 0.5 wt%, 1.0 wt%, and 1.5 wt% of the developed RH-SNP at 1:1 ratio basis were added to the spud mud. These additives were mixed thoroughly in a multi-mixer (20N IKA Rw). The test is to examine the impact of the RH-SNP on the spud mud properties before using the RH-SNP to formulate complex drilling mud systems.

2.2.2.2. Complex drilling muds formulations. After confirming the improvement in the rheological and filtration properties performance of the spud mud with different amounts of RH-SNP, different complex WBMs with RH-SNP were formulated. The formulation was mainly carried out to evaluate the efficiency of RH-SNP material as LCM. The complex WBM system was formulated in ascending order of the additives presented in Table 1 starting with tap water to barite. These additives were mixed thoroughly in a multi-mixer (20N IKA Rw). Finally, 1:1 ratios of different concentrations (0.5–2.0 wt%) of RH-SNP were dispersed in 50 ml of deionized water (DW) and sonicated for 2 h to cause the dispersion of the particles in aqueous solutions. Thereafter, these concentrations were added into the prepared base mud system (Table 2) after the barite mixing time. The mud properties were determined before (80 °F) and after (250 °F) thermal aging process.

2.2.3. Testing protocols

To accomplish the study objectives, different tests were conducted on both the spud muds and complex drilling mud systems. These tests include: (1) investigating the rheological properties of both the spud muds and complex drilling muds, (2) examining the filtrate loss control performance of the various drilling muds, (3) bridging material test with the use of straight slotted filter discs in a fractured formation to understand the impact of RH-SNP in fracture plugging, and (4) potential field applications of the RH-SNP in mitigating lost circulation and possible replacement for industrial nutshell. The description of these tests is summarized next.

2.2.3.1. Rheological characterization using Bingham plastic model. The viscosity-profile of a complex drilling mud was evaluated using a mathematical model by Bingham generally known as Bingham plastic model. Bingham plastic fluid characterization, which remains predominant for description in the field is a two-parameter model, which are the yield stress and plastic viscosity (Oseh et al., 2020a). These two parameters were evaluated to determine if the shear stress surpass a certain point to break the bond gelation of the complex drilling mud and allow it to flow. Test on these parameters were conducted according to the test protocols of American Petroleum Institute (API RP 13B-1., 2017). The rheological characterization test was carried out at 78 °F (without aging) and 250 °F (after aging) the different mud systems in a 4-roller dynamic hot rolling cell by using a Brookfield 8 – speed rotational viscometer

Table 1
Components of formulated complex WBM system used in this study following 1 lab barrel = 350 ml.

Materials	Units	Functions	Concentrations	Mixing time (min)
Tap water	ml	Base fluid	350	–
NaOH	wt.%	pH control	1.60	4.00
Bentonite	wt.%	Viscosity modifier	30.0	10.0
PAC	wt.%	Viscosity and filtrate loss agent	3.00	5.00
$CaCl_2$	wt.%	Density enhancer	28.0	5.00
Na_2CO_3	wt.%	To increase bentonite performance	1.60	5.00
Barite	wt.%	Weighting agent	70.0	30.0

Table 2
WBM system with different concentrations of RH-SNP in a 1:1 ratio basis.

Mud system	Compositions of mud components
Complex WBM	Base mud
0.50 wt% RH-SNP	WBM + 0.50 wt% RH-SNP
1.0 wt% RH-SNP	WBM + 1.0 wt% RH-SNP
1.5 wt% RH-SNP	WBM + 1.5 wt% RH-SNP
2.0 wt% RH-SNP	WBM + 2.0 wt% RH-SNP

(BF45, Middleboro, MA, USA).

The shear stress (τ) values under stabilized shear rates (γ) from 5.11 s^{-1} to 1022 s^{-1} were recorded against eight different dials between 600 rpm and 3 rpm, which are 600 rpm, 300 rpm, 200 rpm, 100 rpm, 60 rpm, 30 rpm, 6 rpm, and 3 rpm. Then, the shear-stress and apparent viscosity (AV) values corresponding to the shear-rate values between 5.11 s^{-1} and 1022 s^{-1} were obtained for two different temperatures of 80 °F (without aging) and 250 °F after aging the mud samples in a 4-roller dynamic oven's aging cell for 16 h. Thus, the shear stress, shear rate, and apparent viscosity were calculated by using equations (1)–(3). Thereafter, plots of shear-rate vs shear-stress and shear-rate vs effective viscosity were made to study the viscosity-profile of the different complex mud samples. The tests were performed thrice to confirm reproducibility and the average values obtained were registered.

$$Shear-rate,\ \gamma\left(\frac{1}{s}\right) = 1.7032 \times N \tag{1}$$

$$Shear-stress,\ \tau\left(lb \Big/ 100ft^2\right) = 1.067 \times \theta \tag{2}$$

$$Apparent\ viscosity,\ AV,\ (cP) = 300 \times \frac{\theta}{N} \tag{3}$$

where N is the rotor speed (rpm); θ is the viscometer dial reading (^{o})

2.2.3.2. Rheological properties measurement of spud muds and complex drilling muds. The procedures undertaken to carry out the experiments on the mud properties (spud muds and complex drilling muds) are briefly discussed. The mud properties (pH, density, plastic viscosity PV, apparent viscosity AV, gel strengths (GS) at 10 s and 10 min, yield point YP) of the spud mud and complex drilling muds were measured. For the spud muds, the tests were conducted at a temperature of only 80 °F, while the temperatures of 80 °F (before aging) and 250 °F (after aging) for 16 h in a 4-roller oven were used in the measurement of the complex drilling mud samples.

For the mud pH measurement, a pH meter was used. The pH meter was standardized with distilled water and the mud sample was poured into a glass beaker. The pH meter probe was dipped into the glass beaker and the pH value at steady position showed on the meter was recorded. Followed next is the mud density measurement.

Mud balance was used to measure the density of the various mud samples. The mud balance was standardized with distilled water. The mud cup was cleaned, dried, and filled to the top with the spud mud sample to be tested. The lid was placed on the cup and some mud was allowed to flow out of the hole on the lid to ensure no trapped air in the cup. The lid and cup were wiped to clean any mud on the surface to get precise measurement. Then, the knife edge was positioned on the fulcrum and the rider adjusted until the mud cup and the rider attained the same balance (equilibrium). Afterwards, the mud density was read on the calibrated arm of the mud balance and recorded.

In terms of rheological properties test, Brookfield 8 − speed rotational viscometer (BF45, Middleboro, MA, USA) was used. The mud sample was poured into the viscometer cup to the scribed line and placed on the viscometer stand and raised to fix the rotating sleeve. With rotor speed set at 600 rpm and 300 rpm (i.e., two-point data measurement), the dial readings of each rpm were recorded at steady values and were used to determine the mud's PV, YP, and AV. 10 s and 10 min GS measurements were performed next. For this test, the rotor speed was fixed at 600 rpm and the mud sample was stirred for 10 s, then, the knob was adjusted to 3 rpm, while the viscometer was immediately switched off to initiate quiescent period for 10 s. Afterwards, the flip toggle was moved to rear (low) position and the maximum dial reading was recorded as the initial gel or 10 s GS. The same process was followed to measure the 10 min GS, but, in this case, the mud sample was permitted to be quiescent for 10 min.

The procedures were repeated to determine the mud properties at 250 °F after thermal aging in a 4-roller oven for 16 h. These methods were followed to determine both the spud mud and complex drilling mud properties. However, only the test of complex drilling muds was extended to 250 °F. All the measurements were conducted in triplicates to establish data precision and reproducibility and their average values were recorded. Thereafter, the PV and YP of both the spud muds and complex WBM systems were fitted using equations (4) and (5), respectively.

$$Plastic\ viscosity,\ PV(cP) = \theta_{600} - \theta_{300} \tag{4}$$

$$Yield\ point,\ YP\left(lb \Big/ 100ft^2\right) = (\theta_{300} - PV) \tag{5}$$

where θ_{600} is dial reading at 600 rpm; and θ_{300} is dial reading at 300 rpm.

2.2.3.3. Filtration properties determination. Filtrate indicates the amount of water lost from the drilling fluid to the reservoir formation, and test of filtration property simulates how much the filtrate loss volume can occur inside the wellbore. Accurate control of filtrate loss can prevent or lessen wall sticking and, in some cases, enhance wellbore stability (Hamad et al., 2020). In the filtration properties test of spud muds and complex drilling muds, Fann API

filter press (series 300) and Fann HPHT filter press (series 3000) were used to measure the API filtrate loss (API FL) and HPHT FL, respectively. However, the measurement of the spud mud was only performed at API condition. The API filtration test was performed at room temperature and 100 psi pressure for 30 min.

The filter press consists of 3-inches ID cylindrical cell and 5-inches height. A sheet of Whatman No. 50 filter paper was fitted at the bottom of the cell and drilling muds were introduced into the measuring cell. The API filter press used contained 6-filter cells mounted on a collective frame. After all the required connections, a 100 psi pressure was supplied to the cells. A measuring cylinder was fixed underneath the cell to collect the filtrate that passes through the filter paper over a 30 min-period and registered in ml equivalent to cm^3 as the API FL. For the HPHT FL measurement, the same procedures were followed, but, in this case, the temperature in the heating jacket was increased to 250 °F and a differential pressure of 500 psi was used. All the tests were performed thrice, and their average values were then recorded.

2.2.3.4. Bridging material test. As experimental works are performed over the years to overcome lost circulation problems, testing devices with similar sealing environments as in the loss formations are developed to simulate the drilling environment for the tests to embody the actual sealing process as close as possible. The API RP Bulletin 13B-1 Specification of Bridging Materials for Regaining Circulation was followed as standard testing protocols to evaluate the capacity of the developed RH-SNP to mitigate lost circulation (Fig. 2). The temperature of 250 °F was applied in the bridging material test cell to achieve a high temperature condition in the drilling process, as suggested by Jeennakorn et al. (2019). A straight slotted filter disk that has the ability to simulate fractures was selected in the screening and evaluation of the developed RH-SNP as potential LCM. The selected slotted filter disk size was applied to simulate 1 mm and 2 mm fractures in the producing formation. The apparatus (Fig. 2) consists of a 6.4 mm × 47.5 mm stainless steel slot disk with a square-edge slot 35 mm in length and a width of 1 mm and 2 mm. It was attached to a graduated (3500 ml) plastic container with an inlet and outlet to accommodate the sudden discharge of the mud cell. The test cell was connected to a pressurized Nitrogen gas to supply pressure on the bridging material test apparatus.

To determine the effectiveness of the additives to prevent lost circulation, the testing process can be abridged into three major steps: seal instigation, seal creation, and seal integrity examination. A 1 mm disk was selected and placed in the valve outlet with perforated plate and sleeves to support the marble bed removed from the cell. Pressurized Nitrogen cylinder valve was opened to the atmosphere and the mud samples were poured into the pressure cell and heated up to 250 °F before running the test. The seal is instigated by adding fluid at a constant flow rate of 25 ml/min for 40 s and terminated at 60 s. The step is repeated until a fast increase in the injected pressure is detected. This increase specifies the seal formation, and the process is continued to create the seal until the pressure goes up to 100 psi. Finally, the seal is created further, and its integrity is tested by adding mud until the pressure increase to 500 psi and then, the injection is stopped for 60 s. This step is repeated, and the pressure is raised by 500 psi each time until the seal fails, and the cylinder was empty. The seal integrity was evaluated after running the tests and the produced seals were removed from the straight slotted filter disk and the final volume was recorded. The procedure was repeated with a slotted filter disk size of 2 mm.

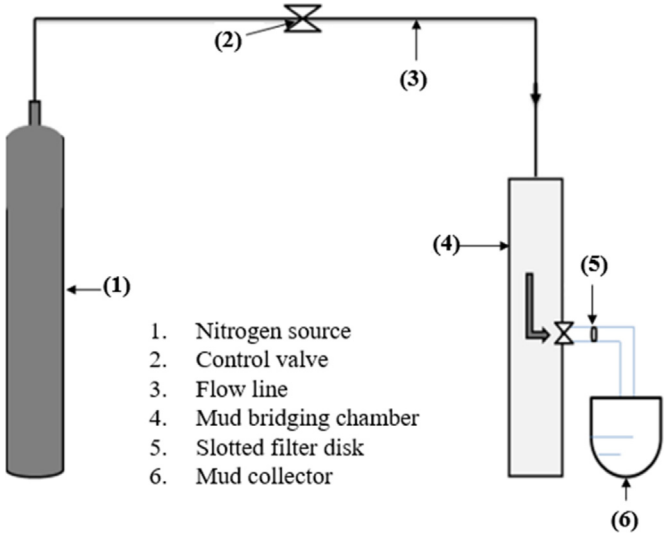

Fig. 2. Simplified bridging material test apparatus.

3. Results and discussions

3.1. Characterization of RH-SNP

The particle size, morphology, and surface structure of the synthesized RH-SNP has been exclusively described in our previous study, and the particle size characterization shows that RH particles size are 3 μm, while RH-SNP has a particle size distribution between 43.9 nm and 59.5 nm (Agi et al., 2020).

3.2. Investigation of spud mud properties

Spud muds are usually applied to commence the drilling of a well. The drilling continues to a few hundred feet of the well. They are mainly applied when surface hole drilling to a shallow depth is recommended (Singh and Dutta, 2018). The results of the properties of unweighted spud muds measured at 80 °F only without aging are shown in Table 3. One of the properties examined is the pH. The analysis of pH is necessary to help in the control of the properties of drilling muds. The mud pH can affect the efficiency of chemicals, solubility, and dispersion of clays. Following Table 3 data, the inclusion of 0.5, 1.0, and 1.5 wt% RH-SNP showed no significant effect on pH of the various spud muds, which ranged from 8.1 to 8.2. By using 0.5 wt% of RH-SNP, the pH was 8.1 and it did not change when 1.0 wt% RH-SNP was used. However, it changes minimally to 8.2 (about 1.2%) with a concentration of 1.5 wt% RH-SNP. This effect is due to the increase in hydroxyl (−OH) ions as larger content of OH ions can alter the liquid pH (Singh and Dutta, 2018).

Table 3
Unweighted spud mud with RH-SNP properties measured at 80 °F (Spud mud: 350 ml tap water + 20 g sodium bentonite + 2.0 g NaOH).

Properties	Spud mud	Concentrations of RH-SNP (wt.%) in spud mud		
	0.0	0.5	1.0	1.5
pH	8.1	8.1	8.1	8.2
Density, ppg	8.4	8.4	8.4	8.4
AV, cP	11	16	21	26
PV, cP	8.0	12	15	19
YP, lb/100 ft^2	6.0	9.0	12	14
10 s GS, lb/100 ft^2	3.0	3.6	4.0	4.1
10 min GS, lb/100 ft^2	4.0	4.5	4.7	5.0
API FL, ml	21	15	13	11

Another important parameter tested is the mud density. The density of the mud influences the hydrostatic pressure in the well and prevents undesired flow into the borehole. Table 3 presents the data of the density of the formulated spud mud with different amounts of RH-SNP. According to Table 3, the introduction of different amounts of RH-SNP showed no changes in the density of the spud mud, which remains constant at 8.4 ppg. This implies that the RH-SNP is unable to induce solid build up in the well (Oseh et al., 2020a).

Also presented in Table 3 is the rheological parameters (viscosities – AV and PV, YP, GS) and API filtrate loss data. From Table 3, the rheological parameters of the spud muds are enhanced as the concentration of RH-SNP increases. For the AV, the data with RH-SNP are 16, 21, and 26 cP with 0.5, 1.0, and 1.5 wt% RH-SNP, which are relatively superior to the base mud (11 cP) by 45.5%, 91%, and 136.4%, respectively. Similarly, the PV data of 12, 15, and 19 cP of 0.5, 1.0, and 1.5 wt% RH-SNP are larger than that of the base mud (of 8 cP) by 50%, 88%, and 138%, respectively. The inclusion of RH-SNP causes the particles to embed in the pore structure of bentonite particles thereby interacting with the clay particles to increase the intermolecular strength of the spud mud. This act assuredly will increase the PV of the liquid (Oseh et al., 2020a; Blkoor et al., 2021; Blkoor et al., 2022). Next is the YP results of the spud mud of 6 lb/100 ft^2. By using 0.5, 1.0, and 1.5 wt% RH-SNP concentrations, the YP of the spud mud improved to 9.0, 12.0, and 14.0 lb/100 ft^2, respectively. This corresponds to an increment of 50%, 100%, and 133%, respectively over that of the base mud. Furthermore, the 10 s gels with RH-SNP amounts of 0.5 wt% (3.6 lb/100 ft^2), 1.0 wt% (4 lb/100 ft^2), and 1.5 wt% (4.1 lb/100 ft^2) exceed that of the base mud (of 3.0 lb/100 ft^2) by 20%, 33.3%, and 36.7%, respectively. Similarly, the 10 min gels for 0.5 wt% (4.5 lb/100 ft^2), 1.0 wt% (4.7 lb/100 ft^2), and 1.5 wt% (5.0 lb/100 ft^2) are superior to the 10 min gel of the base mud (of 4.0 lb/100 ft^2) by 12.5%, 17.5%, and 25%, respectively.

For the API FL data, The API FL of the spud mud (of 21 ml) reduced with all the concentrations of RH-SNP. With the concentrations of 0.5 wt% (15 ml) and 1.0 wt% (13 ml), RH-SNP decreased the filtrate loss volume of the base mud (of 21 ml) by 29% and 38%, respectively. The decrease was more with the 1.5 wt% RH-SNP (11 ml) by 48% due to its higher content in the mud (Oseh et al., 2020b). Also, the evaluated RH-SNP was able to combine with the clay particles (bentonite) to effectively migrate into pores and provide pore clogging (Oseh et al., 2020b). Given the results shown in Table 3, it can be concluded that RH-SNP possesses the ability to enhance the spud mud properties and could serve as lost circulation treatment agent. Thus, RH-SNP was exclusively studied as a potential lost circulation additive.

3.3. Bingham plastic fluid characterization

For better representation of Bingham plastic model, the rheological characterization of a fluids in terms of shear stress, shear rate, and apparent viscosity provide a suitable approximation of the likely flow rates required (Kumar and Savari, 2011). Also, for the purpose of treating drilling fluids, this model could be superior to other models as it specifies the nature of contamination of the drilling fluid and the needed treatment. For example, increasing PV of fluid suggests solid contamination, whereas increasing YP indicates chemical contamination (Jeennakorn et al., 2019). Meanwhile, the Bingham plastic model have been globally accepted because of its simplicity and ability to approximate pressure losses in a turbulent condition with accuracy matching the other rheological models (Jeennakorn et al., 2019). Fluids obeying the Bingham plastic model possess a linear shear stress – shear rate character after the threshold of the initial shear stress (YP) is exceeded, and can be described by the approximation given in equation (6), which confirm the accuracy of Bingham plastic model shown in Fig. 3.

$$\tau = YP + PV(\times \gamma) \tag{6}$$

where, τ = shear stress (lb/100 ft^2); YP $\equiv \tau_o$ is the threshold stress (intercept), (lb/100 ft^2); PV (cP) represents the slope of the line; and γ = shear rate (1/s).

Fig. 3 shows the viscosity character of complex drilling mud with RH-SNP at 78 °F (Figs. 3a) and 250 °F (Fig. 3b) tested under different shear rates in a log-log graph fitted by Bingham plastic model. The rheogram confirmed an increment in the shear stress of the base mud with an increasing shear rate when the amounts of RH-SNP were added. Also, the trend lines shown in Fig. 3 revealed that the mud resists flow initially until the shear stress surpasses a certain point. This interprets the visco-plastic nature of a Bingham plastic fluid, in that the fluid acts as a rigid body at low shear stress but flows as a viscous fluid at high shear stress (Elochukwu et al., 2017). This plot is similar to the description of Bingham plastic fluid by Elochukwu et al. (2017).

Further, Fig. 4 (a: T = 78 °F; b: T = 250 °F) presents the viscosity-profile result of AV under different shear rates fitted with Bingham plastic model. It was found that both the hot-rolled and drilling muds without hot-rolled displayed a quite similar rheological character. The AV values of the RH-SNP are decreased with increasing shear rates. This behaviour confirms non-Newtonian character of the mud samples. Like most polymers, the RH-SNP shows pseudoplastic behaviour, which can be explained by the particles of RH-SNP tendency to align with each other at high shear rates leading to easier flow from lowest shear rate of 5.11 s^{-1} to highest shear rate of 1022 s^{-1} (Alsaba et al., 2014). This character allows drilling fluid to suspend drilled solids and cuttings when the fluid circulation halts. Observation from Fig. 4a and b further show that addition of 2.0 wt% of RH-SNP to the complex drilling mud systems indicates greater impact on the viscosity-profile at both 78 °F and 250 °F, which is a function of the amount of the RH-SNP (Ghosn et al., 2017; Oseh et al., 2020b). These plots further showed that the evaluated drilling muds behave like a Bingham plastic mud and the trend lines are consistent with the recent findings by Oseh et al. (2020b).

3.4. Effect of RH-SNP on rheological properties of complex drilling mud

The rheological parameters of the complex drilling mud may be affected with the inclusion of RH-SNP. Therefore, it was deemed fit to examine the impacts of RH-SNP concentrations on the rheological behaviour of the complex drilling mud. Tables 4 and 5 show the rheological and fluid loss characteristics of the complex WBM system with different concentrations of RH-SNP with and without heating.

3.4.1. Mud pH

Tables 4 and 5 show the pH values of the conventional WBM and RH-SNP drilling mud systems at 80 °F and 250 °F, respectively. At 80 °F (Table 4), the pH values of the WBM slightly changed with the addition of 0.5, 1.0, 1.5, and 2.0 wt% RH-SNP between the ranges of 8.5 and 8.9 by 0%, 2%, 2%, and 4.7%, respectively, mainly because of the aggregation character of the RH-SNP; the growth of NPs can alter the pH of drilling muds (Oseh et al., 2020b). After exposing the mud samples to high temperature of 250 °F (Table 5), the pH of the WBM with the RH-SNP increased with the concentration of RH-SNP but showed a decreasing trend from 0.5 wt% to 2.0 wt% in the range of 23.7% and 2.4%, respectively. These values are higher than those

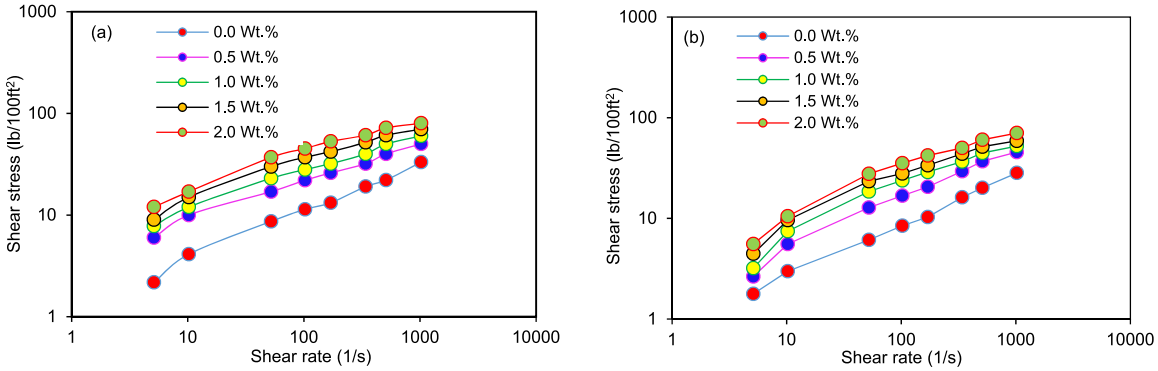

Fig. 3. Shear stress versus shear rate of complex WBM with RH-SNP (a: T = 80 °F; b: T = 250 °F).

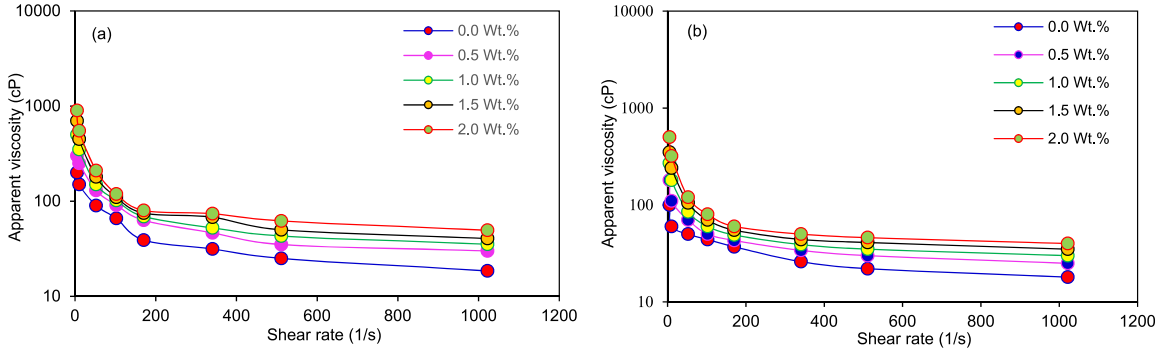

Fig. 4. Shear stress versus apparent viscosity of complex WBM with RH-SNP (a: T = 80 °F; b: T = 250 °F).

Table 4
Rheological properties of complex WBM with different concentrations of RH-SNP at 80 °F.

Properties	WBM	Concentrations of RH-SNP (wt.%) in WBM at 80 °F			
	0.0	0.5	1.0	1.5	2.0
pH	8.50	8.50	8.67	8.67	8.90
Density (ppg)	9.50	11.5	11.6	11.7	11.8
AV (cP)	13.0	25.5	33.0	41.0	44.5
PV (cP)	7.00	19.0	24.0	31.0	34.0
YP (lb/100 ft^2)	12.0	15.0	18.0	20.0	21.0
GS (10 s) (lb/100 ft^2)	6.00	800	9.00	10.0	10.0
GS (10 min) (lb/100 ft^2)	6.00	8.00	9.50	11.0	11.0

found at ambient temperature conditions. This is because, with an increase in temperature, molecular vibration and movement of the particles increased, causing the particles to have fewer hydrogen ion present. Thus, the more hydrogen ions, the lower the pH. Conversely, the fewer hydrogen ions, the higher the pH (Rajesh et al., 2016; Lohrasb et al., 2021).

Table 5
Rheological properties of complex WBM with different concentrations of RH-SNP at 250 °F.

Properties	WBM	Concentrations of RH-SNP (wt.%) at 250 °F			
	0.0	0.5	1.0	1.5	2.0
pH	8.50	9.87	8.96	8.80	8.70
Density (ppg)	9.20	11.2	11.4	11.4	11.5
AV (cP)	12.5	23.5	31.0	36.0	43.5
PV (cP)	7.00	17.0	22.0	26.0	33.0
YP (lb/100 ft^2)	11.0	13.0	18.0	20.0	21.0
GS (10 s) (lb/100 ft^2)	6.00	7.00	8.50	9.00	9.00
GS (10 min) (lb/100 ft^2)	6.00	9.00	9.00	10.0	10.0

3.4.2. Mud density

Tables 4 and 5 present the density of conventional WBM with different concentrations of RH-SNP. As shown in Table 4, the density of the WBM (of 9.3 ppg) increases with an increasing concentration of the RH-SNP between 11.5 and 11.8 ppg before aging, which is due to more solids accumulation when the amount of the RH-SNP is increased (Fattah and Lashin, 2016). Thus, the density of the base mud increases with 0.5, 1.0, 1.5, and 2.0 wt% by 23.7%, 24.7%, 25.8%, and 26.9%, respectively. After aging (Table 5), the density of the WBM (of 9.2 ppg) also increases with an increasing concentrations of the RH-SNP between 11.2 and 11.5 ppg by 21.7% and 25%, respectively. Moreover, these densities are reduced compared to those before aging shown in Table 4, which interprets the weakening of the RH-SNP particle-mud interactions caused by heat disruption of the particles (Fattah and Lashin, 2016). Nevertheless, the observed reduction in the densities of the RH-SNP mud samples is minimal and it will not lead to wellbore collapse and underbalanced well condition. An underbalanced well condition implies that formation fluids, such as water, oil, or gas will enter the drilled formation to impair the drilling process, such as problems of differential pipe sticking (Blkoor et al., 2021).

3.4.3. Apparent viscosity

The AV of RH-SNP was determined and compared with the base mud (Tables 4 and 5). The AV = 13 cP of the WBM (Table 4) reduced slightly after thermal aging (AV = 12.5 cP) (Table 5), which is

attributed to high bentonite content flocculation in the base mud (Table 1). The AV result is consistent with a more recent study by Blkoor et al. (2022) wherein the authors stated that, a fluid with a high content of bentonite exposed to hot rolling in the oven promotes the formation of gel structure which increases the AV. However, the RH-SNP content increases the AV before and after thermal aging. The AV (25.5, 33, 41, and 44.5 cP) of the RH-SNP in WBM showed high margins of increment with an increasing concentration (0.5, 1.0, 1.5, and 2.0 wt%) of the RH-SNP, respectively. At the lowest concentration of 0.5 wt% RH-SNP, the AV of the WBM is increased by 96.2%. The highest margin of increase in the AV of the WBM (242.3%) was observed with 2.0 wt% RH-SNP, while 1.0 and 1.5 wt% RH-SNP enhanced the AV by 153.8% and 215.4%, respectively. The increasing trend of the AV of the WBM with the RH-SNP is due to the small size of the RH-SNP particles that were mainly distributed within the nanometer domain (43.9–59.5 nm). This caused increased internal friction between the particles and absorbed water molecules (Oseh et al., 2020d).

The impact of high temperature is a good indicator to ascertain the temperature resistance of additives under the bottom-hole conditions. Typically, drilling muds often displayed a reduction in viscosities (AV and PV) and YP with an increase in temperature, as evident in this study after thermal aging (Table 5). According to Table 5, the AV of the RH-SNP showed a little lower decrease in the WBM than the AV displayed in Table 4 except at 2.0 wt% of RH-SNP, where it improved the base mud by 248%. This could be attributed to the excellent heat resistance of the RH-SNP, whose structure remained stable during thermal aging even at higher concentrations (Saleh and AL-Hammadi, 2018). At concentrations of 0.5–2.0 wt% RH-SNP, the AV of the base mud (of 12.5 cP) improved with aging between 12.5 cP and 36 cP by 88%, 148%, 188%, and 248%, respectively (Table 5). This shows the impact of encapsulation of the mud; this breakpoint differs with molecular weight and with solids in the mud. This slight decrease is due to the weakening of the intermolecular forces in the mud samples (Ismail et al., 2016). Given the AV data displayed in Tables 4 and 5, it can be inferred that the RH-SNP will be suitable for fluid motion and stability, especially in a high-temperature environment.

3.4.4. Plastic viscosity

PV prevents leakage of drilling mud into formation adjoining the wellbore. Therefore, the impact of RH-SNP on PV of the conventional WBM was determined (Tables 4 and 5). The WBM showed a constant value of PV at 7 cP both before and after thermal heating. The principle behind the viscosity of the WBM is the ability of the molecules of water to interact directly with polymeric chains and other additives via hydrogen bonds with its hydrophilic groups. This increases their intermolecular forces resulting in the viscosity (Saleh and AL-Hammadi, 2018). The addition of 0.5, 1.0, 1.5, and 2.0 wt% RH-SNP significantly increased the PV (to 19, 24, 31, and 34 cP) of the WBM system, respectively, which could be attributed to the effective dispersion and distribution of RH-SNP and its contact with water molecules (Gbadamosi et al., 2019a). With increasing concentration of RH-SNP, the PV values were of the base mud are increased by 171.4%, 242.9%, 342.9%, and 385.8%, respectively (Table 4).

The increase in the PV of the base mud with RH-SNP is due to the effective contact and distribution of the particles with WBM molecules that increases the stability of RH-SNP (Wang et al., 2012). Also, increasing amount of RH-SNP unites the RH-SNP on bentonite clay plates, increasing the linking among the clay layers and preserving the forces of attraction between the clay plates (Medhi et al., 2020). Similarly, the PV of the WBM improved with RH-SNP concentrations between the ranges of 17 and 33 cP by the range of 142.9%–371.4% after thermal heating (Table 5). Amount of 2.0 wt % of the RH-SNP showed higher impact on the PV of the complex drilling muds at both 80 °F and 250 °F temperatures owing to its higher amount in the mud. This phenomenon also implies that the RH-SNP product had induced a thinning behaviour at lower amounts and a gelling character at higher amounts on the drilling mud (Medhi et al., 2020), exemplifying the accuracy of the Bingham plastic model used to fit the fluid properties. The PV values shown in both Tables 4 and 5 could be preferred for drilling practice, indicating that the addition of RH-SNP can withstand high-temperature environments, since the PV of the NPs-based mud is strongly affected by the solids and clays available in the mud.

The results presented in Tables 4 and 5 show that the inclusion of RH-SNP causes an increase in PV compared to the PV of the base mud. PV is a measure of the resistance to fluid flow caused by mechanical friction (Blkoor et al., 2021). An increase in solids content, an increase in the overall surface area of solids exposed, and a decrease in the size of solid particles will help to increase the PV. According to the report of Saleh and AL-Hammadi (2018), large specific surface area per volume of NPs that increases the interaction site, high surface forces including electrostatic and van der Waals forces that increase its intermolecular strength with WBM, and extremely small size that enable it to fit into tiny pores and function effectively are the main determinants of NPs for outstanding properties. These factors increase their interaction sites with drilling mud matrix (Saleh and AL-Hammadi, 2018).

In the complex drilling mud, synergistic effect of PAC and RH-SNP could provide desirable fluid properties required for drilling. The RH-SNP can bond with nonionic cellulose compound, such as PAC having –OH groups to cause an increase in the average molecular weight so as to absorb on the surface of the clay particles and help the particles to attach to each other. This can result in an increase in the intermolecular strength of the particles, subsequently causing an increase in the liquid viscosity (Fereydouni et al., 2012). Also, RH-SNP through its cellulosic component can link or bond directly through an intermediary chemical association with the drilling mud matrix, resulting in an increased PV (Fereydouni et al., 2012).

3.4.5. Yield point

The YP indicates the ability of drilling fluid to carry drilled cuttings or rock debris to the surface. Therefore, it signifies the potency of the mud to avoid pipe sticking problems. Tables 4 and 5 show the effect of RH-SNP concentration on the YP of WBM before and after aging. The results show that the YP of the WBM increased as the concentration of RH-SNP increases. This could be because of the extremely small size of the RH-SNP that resulted in a high surface area, that acts as a site for bonding by interacting with other mud molecules; thereby, creating a rigid network for the YP improvement (Elochukwu et al., 2017). The addition of 0.5, 1.0, 1.5, and 2.0 wt% RH-SNP improved the YP = 12 lb/100 ft^2 of the WBM system to 15, 18, 20, and 21 lb/100 ft^2 by 25, 50, 66.7, and 75% at 80 °F, respectively (Table 4). The increase in YP of the base mud with RH-SNP (Table 4) indicates that the YP of the base mud is affected by the presence of the RH-SNP. This shows a strong interaction between the RH-SNP with the base mud molecules to form a reticular structure, which is as a result of the electrostatic attraction between the negatively charged RH-SNP and positively charged edges of the bentonite particles (Ngouangna et al., 2020; Bao et al., 2019).

It can also be seen in Table 5 that the addition of RH-SNP increased the YP = 11 lb/100 ft^2 of the base mud after aging by 18% (13 lb/100 ft^2) with 0.5 wt% to a higher margin of increment with 1.0 wt% by 63.6% (18 lb/100 ft^2). It then increases more by 81.8% and 90.9% with 1.5 wt% (20 lb/100 ft^2) and 2.0 wt% (21 lb/100 ft^2), respectively. The driving principle behind the increased

performance of the YP of the mud samples of RH-SNP is because of the reduced interparticle space that confines the repulsion capacity and supports the coagulation of the RH-SNP (Oseh et al., 2020a; 2020b). Following the YP levels which have to be from 10 to 45 lb/100 ft^2, as recommended by API standards (API RP 13B-1., 2017), the concentrations of the RH-SNP product could be an ideal candidate for efficient cuttings transport and wellbore cleaning. Therefore, it is inferred that along with the increase in AV, PV, and YP, the RH-SNP displayed a substantial degree of thermal resistance at increasing concentration. If this feature continues to hold at low concentrations ($\leq 2.0\ wt.\%$) for even at higher temperatures, not only will it save drilling costs, but will also contribute immensely to the drilling of HPHT environments.

3.4.6. Gel strength at initial and 10 minutes

The behaviour of drilling mud when drilling is stopped or paused is determined by its GS. Hence, the optimum gel composition is ideal to carry drill cuttings efficiently and to avert barite sag. The influence of RH-SNP concentration on the GS of reference mud is shown in Tables 4 and 5 Besides, detecting an increase in GS (initial and 10 min) in these tables with the amounts of RH-SNP, the RH-SNP also contains the characteristic of temperature resistance that assisted to preserving the GS when the mud was circulated at bottom-hole environments. This character will guarantee appropriate suspension of barite and drilled cuttings thus averting sagging problems (Boyou et al., 2019). The increase in the 10 s GS of the WBM (of 6 lb/100 ft^2) to 8 lb/100 ft^2 by 33.3% with RH-SNP occurred when 0.5 wt% was added. At 1.0 wt% RH-SNP, the gel improved to 9 lb/100 ft^2 by 50% and remained unchanged (10 lb/100 ft^2) by 66.7% with 1.5 and 2.0 wt%. For the 10 min gel test conducted, the gel of the base mud before and after aging is constant at 6 lb/100 ft^2; it increases with an increasing amount of RH-SNP. At 0.5, 1.0, and 1.5 wt% RH-SNP, the gels increased to 8 lb/100 ft^2 by 33.3%, 9.5 lb/100 ft^2 by 58.3% and 11 lb/100 ft^2 by 83.3%, respectively; then remain constant at 2.0 wt% (11 lb/100 ft^2 by 83.3%) (Table 4). After aging, it increases by the same margin of 50% to 9 lb/100 ft^2 with 0.5 and 1.0 wt% RH-SNP before increasing again by the same margin of 66.7% to 10 lb/100 ft^2 with 1.5 and 2.0 wt% RH-SNP (Table 5). This implies that RH-SNP can improve the viscosity of the gel which resulted in three-dimensional network structures (Wang et al., 2012).

The GS of the WBM was strengthened by the addition of RH-SNP into the mud solution, which led to linking with the WBM molecules within the 10 s and 10 min period to form a rigid network. This event will surely improve the gel property (Oseh et al., 2020d). Also, the presence of −OH on the surface of the RH-SNP formed hydrogen bonds with the water molecules for improved properties (Oseh et al., 2020d). Furthermore, RH-SNP are negatively charged and the hydronium ions are bounded by electrostatic attraction; thus, a higher water-bound ratio was created by the hydrogen bonds and electrostatic attraction, prompting better gel hydrophilicity (Chen et al., 2013). This contributed to improved suspension capacity and thermal stability of the mud gel. Tables 4 and 5 pertaining to the GS at both temperatures of 80 °F and 250 °F show that the variation between the initial and 10 min GS of the RH-SNP are below 5.0 lb/100 ft^2 which is not much to cause recirculation difficulties after prolonged quiescent period (static condition). The seeming benefit of the RH-SNP product for drilling jobs is its efficient temperature resistance and stability under the bottom-hole conditions of HPHT.

3.4.7. Filtration properties

Filtrates loss behaviour of basic mud depends on the type and quantity of colloid materials in the fluid. Hence, better filtrate loss-control can be achieved when a substantial quantity of colloid materials is included. Figs. 5 and 6 show the effect of RH-SNP concentration on filtrate loss volume before and after aging, respectively. The results show that the addition of RH-SNP decreased the filtrate loss volume compared to base mud (Fig. 5). This signifies the strength of the RH-SNP to transport into pores not accessible by larger particles to combat filtrate loss (Okon et al., 2014). RH-SNP has the ability to induce interaction in the mud by cross-linking with other mud particles, such as sodium bentonite. It can reduce the permeability of the bentonite particles by strengthening the edge-to-edge and edge-to-face bond interactions between the particles, which ultimately will result in reduced fluid loss volume and improvement in rheology (Medhi et al., 2020; Blkoor et al., 2022).

For the RH-SNP mud samples, the inclusion of 0.5 and 1.0 wt% after testing for 30 min under API condition decreased the filtrate loss from 19 ml of WBM to 15 ml and 14 ml by 21% and 26%, respectfully. Similarly, the inclusion of 1.5 wt% minimized the amount of filtrate loss of the base mud to 12 ml by 37%. The filtrate loss was best reduced with 2.0 wt% of the RH-SNP to 10 ml by 47%. This decrement occurred as the RH-SNP block the pore spaces that would have permitted a clear passage of the muds; a benefit of NPs due to their narrow size particles distribution (Oseh et al., 2019a; 2019b). Furthermore, a better sealing performance at higher amounts of RH-SNP was observed. This is because, at lower amounts, the RH-SNP cannot effectively interconnect with each other seamlessly to form a compact film that can prevent the fluid from seeping into the reservoir formation (Xuan et al., 2014). As such, at lower amounts, only a few sheets can contact each other, resulting in a large void in the filter cake (Fig. 5), whereas, at higher amounts, the closely packed sheets can interlock together to effectively minimize the amount of fluid seeping into the reservoir formation (Xuan et al., 2014).

A temperature increase can cause a reduction in the liquid phase viscosity thereby leading to increased filtrate loss; however, the impact of high temperature was not felt in the base mud and is not significant in the RH-SNP mud samples, owing to their efficient thermal stability and dispersion. After aging (Fig. 5), the effect diminished a little, but the outcome was still within the recommended range of field practice for high temperature conditions (API RP 13B-1., 2017). For the 0.5 wt%, 1.0 wt%, 1.5 wt%, and 2.0 wt% RH-SNP in the base mud, the filtrate loss control was improved to 16 ml, 14 ml, 12 ml, and 11 ml by 16%, 26%, 37%, and 42%, respectively. This shows that when the base mud goes through some thermal treatment at 250 °F, it was stabilized by the RH-SNP. This property can help the RH-SNP to withstand hot drilling environments and be effective for sealing, minimizing fines and mud migration into the drilled formation (Xuan et al., 2014). Commenting further on the

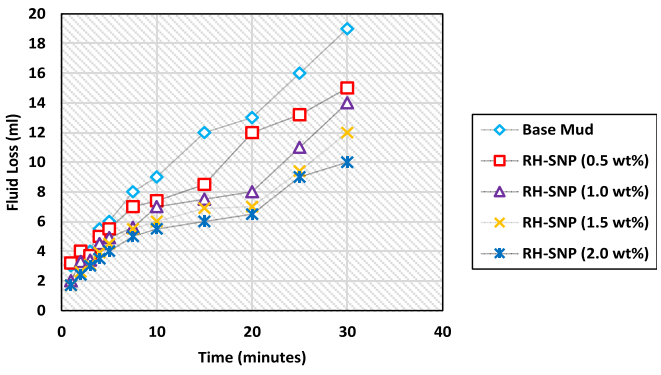

Fig. 5. Fluid loss of complex WBM with RH-SNP (Time = 30 min, Temperature = 80 °F, differential pressure = 100 psi).

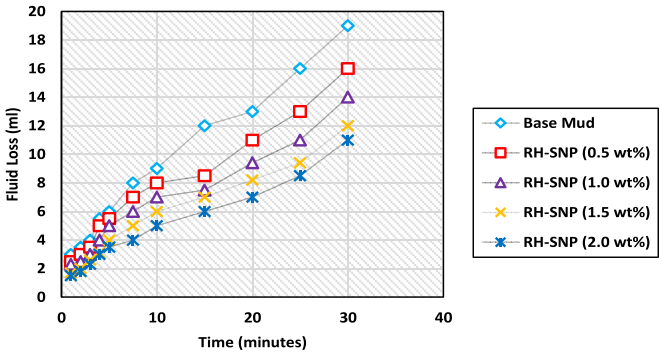

Fig. 6. Fluid loss of complex WBM with RH-SNP (T = 30 min; Temperature = 250 °F; differential pressure = 500 psi).

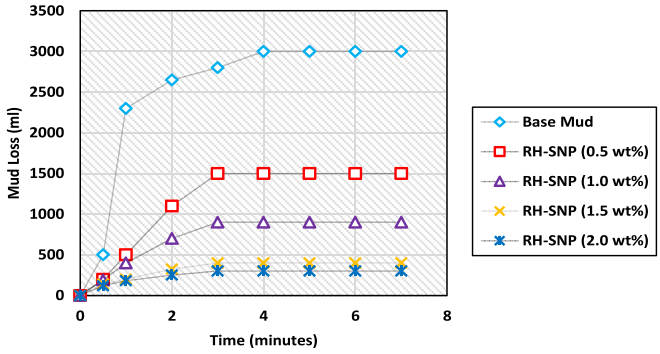

Fig. 7. Mud loss of complex WBM with RH-SNP in 1 mm simulated fracture for 7 min (T = 250 °F; P = 500 psi).

results shown in Tables 5 and 6, the RH-SNP drilling fluids were observed to contain higher YP, which is advantageous for cuttings transport and hole cleaning. They also showed desirable viscosities (AV and PV) and low fluid loss volume compared to the base mud; these attributes are beneficial for fast fluid motion and mitigation of lost circulation.

Overall, the results of filtrate loss control shown in Fig. 5 (unaged muds) and Fig. 6 (aged muds) showed that the introduction of RH-SNP effectively minimized the seepage of fluid into the drilled formation. This event resulted because of the synergistic effect between the RH-SNP and the modified natural PAC acting as a filtrate loss control agent in the drilling mud. The evaluated RH-SNP has high surface area per volume ratio and was dispersible in water; hence, is able to bond or link directly with the water soluble and freely dispersible PAC molecules through the −OH groups along the PAC chain to possibly clog the pore spaces of the filter paper and permit less filtrates to seep through its hydrophilic layer. Consequently, decreasing the filtrate loss volume of the mud (Fereydouni et al., 2012; Hamad et al., 2020).

3.4.8. Loss circulation evaluation of RH-SNP

Stainless-steel slotted filter disk was used to simulate rock matrix in a fractured formation to mimic the production zone. The performance evaluation of RH-SNP in controlling loss circulation at different concentrations with the stainless-steel disk was determined. Fig. 7 shows the mud loss volume of RH-SNP at different concentrations compared to the base mud in a 1 mm simulated fracture. The result shows that RH-SNP minimized the fluid floss better than the base mud and the performance increases with an increasing concentration of the RH-SNP. The mud loss volume of the base mud reduced by 50, 66.7, 86, and 90% with the inclusion of 0.5, 1.0, 1.5, and 2.0 wt% of RH-SNP, respectively. This is because many particles moved into the fracture at the same time and gather effortlessly at the fracture entry point to complete the linking, plugging, and shutting process (Alsaba et al., 2014). Also, the addition of RH-SNP fibres might have increased the shear stress of the plugging zone. The result is consistent with the earlier work of Okon et al. (2014), they reported that the cohesive force and inner friction point increases drastically when fibres are added, as fibre can enhance the shear strength of drilling fluids.

Table 6
Elastic modulus and poisson's ratio of RH-SNP and nutshell as lost circulation agents.

Material	Elastic Modulus E (GPa)	Poisson's Ratio
RH-SNP	66.3–74.8	0.15–0.19
Nutshell	10.0–20.0	0.40–0.50

Fig. 8 shows the mud loss of RH-SNP at different concentrations compared to the base mud in a 2 mm simulated fracture. The result shows that RH-SNP still retained its better sealing ability than the base mud, but its effect on the base mud to seal the fracture formation is lower compared to the 1 mm fracture. With 0.5, 1.0, 1.5, and 2.0 wt% of RH-SNP, the mud loss volume of the base mud reduced by 40, 65.7, 77.1, and 80%, respectively. As the fracture is increased to 2 mm, the void spaces within the fracture increased as the base mud failed and could no longer control the mud loss (Fig. 8). Moreover, the addition of RH-SNP resulted in particle overlap to form a RH-SNP network in the void spaces (Wang et al., 2012). The RH-SNP network supported the sealing network under exterior weight and the three-dimensional reinforcement impact of RH-SNP improved the potency of the seal (Wang et al., 2012). However, since the 2 mm fracture was larger compared to the 1 mm, it took a longer time for the RH-SNP to fill the empty spaces to improve the efficiency of the seal to reduce the mud losses.

3.4.9. Effect of particle size on loss circulation

To regain or minimize fluid loss into the formation, materials for lost circulation in the drilling mud must function in such a manner that the mud's particles has to increase in size to clog the pores and cracks that mud alone cannot clog (Alsaba et al., 2014; Jeennakorn et al., 2019). Materials for lost circulation in drilling mud should possess certain particle size. For illustration, if the LCM is of a very large particle size for a given fracture width, the particles will find it very difficult to go into the fracture. Thus, pore and crack clogging will not occur. Similarly, if the LCM is of a very small size, the particles will pass via the fractures and particle bridging may never take place (Wang et al., 2012; Bao et al., 2019). Therefore, the particle size of materials for lost circulation treatment and their

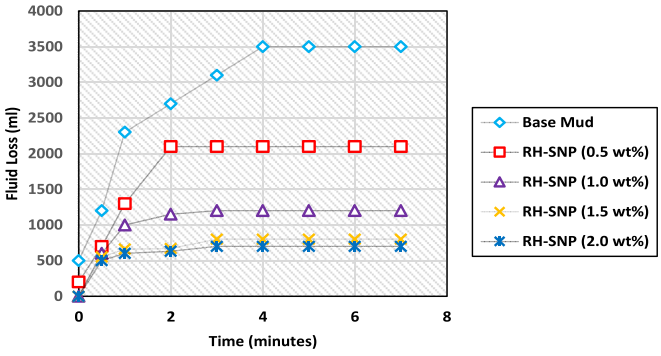

Fig. 8. Mud loss of complex WBM with RH-SNP in 2 mm simulated fracture for 7 min (T = 250 °F; P = 500 psi).

distributions are very vital to seal fractures properly and very fast.

The effect of particle size (3 μm and 43.9–59.5 nm) at the same concentration 1.0 wt% on loss circulation of a 1 mm simulated fractured formation was determined and the result was shown in Fig. 9. The result shows that the fluid loss is decreased as the size decreases. This could be attributed to a surge in the quantity of particles in solution and subsequently, boosting the likelihood of interaction between the particles (Kumar et al., 2021). Also, significant enhancement in the heat and mass transfer of the RH-SNP is possible due to micro-convention and mechanical agitation that are induced by the Brownian motion of RH-SNP in the base fluid (Wang et al., 2012).

Fig. 10 shows the effect of particle size in a 2 mm simulated fracture. The result shows a higher fluid loss for base mud and RH compared to RH-SNP. This could be attributed to the large particle size of the base mud and RH (with a size of 3 μm), thereby, causing additional empty spaces inside the seal (Hamad et al., 2020). The narrow particle size distribution of RH-SNP (43.9–59.5 nm) showed the lowest fluid loss because of the particle's ability to easily fill up the void spaces (Okon et al., 2014). Accordingly, the increase in particle size increases the possibilities of clustering and aggregation which decreases the thermal ability of the particles, as observed with the base mud and particle size of 3 μm.

4. Field application of the experimental results

The reason for this analysis is to determine how efficient is the developed RH-SNP when used to control filtrate loss and lost circulation. This analysis is presumed to indicate the decrease in filtrate loss that the driller will observe once the fracture is sealed effectively. The filtrate loss into the fractured formation that the seal can hold with time was evaluated and compared with conventional nutshell used in the industry at the same concentration of 1.0 wt%. A total time of 7 min was used to study the seal integrity of the various mud systems which falls within the range of previous research by Alsaba et al. (2014). These authors conducted similar research using five different sealing time of 100s ≅ 1.67 min, 150s ≅ 2.5 min, 200s ≅ 3.33 min, 250s ≅ 4.17 min, and 300 s ≅ 5 min. The results from this test are shown in Figs. 11 and 12 for 1 mm and 2 mm simulated fractures, respectively.

The results (Figs. 11 and 12) show that RH-SNP provided better performance compared to conventional LCM at both simulated conditions (1 mm and 2 mm fracture). The highest decrease in the fluid loss of RH-SNP compared to the nutshell and base mud is due to the fact that the RH-SNP has the smallest particle size compared to the nutshell and the base mud. The more deformation of the nutshell than the RH-SNP shown in Table 6 is another reason (Wang et al., 2012). The deformation of a material depends on its elastic

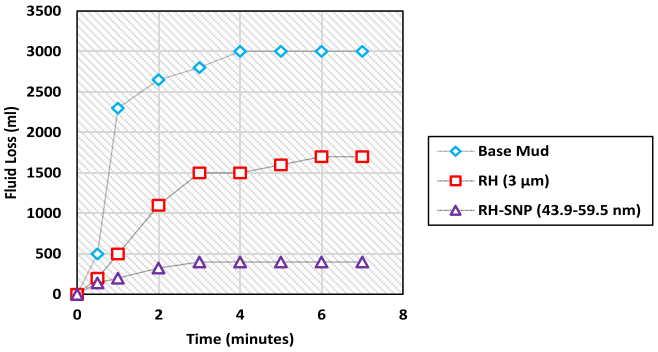

Fig. 9. Effect of particle size of complex WBM and RH-SNP mud samples on loss circulation in a 1 mm simulated fracture for 7 min (T = 250 °F; P = 500 psi).

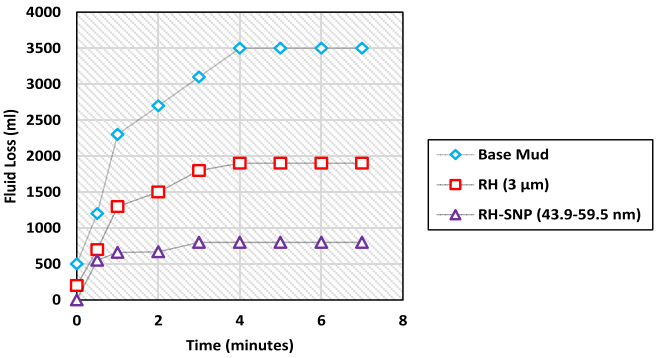

Fig. 10. Effect of particle size of complex WBM and RH-SNP mud samples on loss circulation in a 2 mm simulated fracture for 7 min (T = 250 °F; P = 500 psi).

modulus. The higher the elastic modulus of material, the greater the intensity and stability, and it does not collapse easily (Wang et al., 2012). Table 6 shows the elastic modulus of RH-SNP and nutshell. The elastic modulus of RH-SNP is larger than that of nutshell, and as such was able to withstand the local deformation (Ghalambor et al., 2014; Hamad et al., 2020). With the nutshell, the fracture was bridged and the wall provides weak frictional support that could not hold the particles in place. In compressional stress, bridging particles are deformed at the point of contact between the particle and the wall, resulting in a loose frictional force. This deformation weakens the strength of the particles and parted

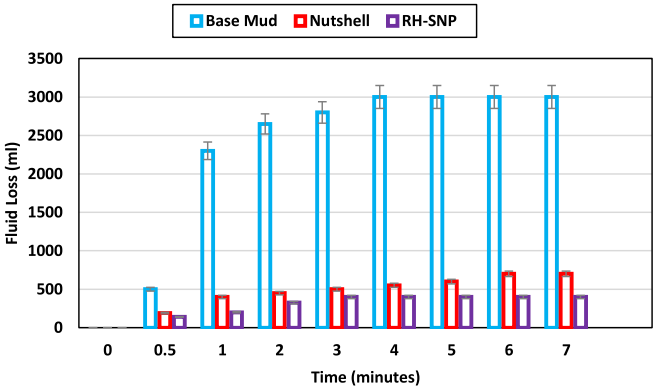

Fig. 11. Total fluid loss of complex WBM, RH-SNP, and nutshell in a 1 mm simulated fracture for 7 min (T = 250 °F; P = 500 psi).

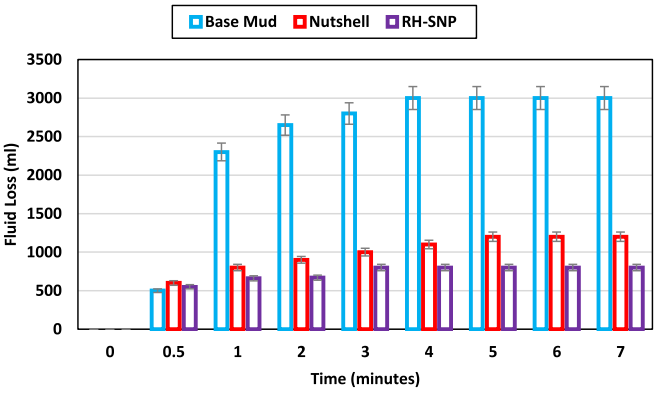

Fig. 12. Total fluid loss of complex WBM, RH-SNP, and nutshell in a 2 mm simulated fracture for 7 min (T = 250 °F; P = 500 psi).

Table 7
Comparison of cumulative percent change in filtrate loss with respect to time for a 1 mm fracture of drilling muds (Time = 7 min; T = 250 °F; P = 500 psi).

	Nutshell mud system								RH-SNP mud system							
	0.50	1.0	2.0	3.0	4.0	5.0	6.0	7.0	0.50	1.0	2.0	3.0	4.0	5.0	6.0	7.0
% Change in filtrate loss	60	83	83	82	82	80	77	77	70	91	87	86	88	87	87	87
Enhancement	Yes	Yes	Yes	Yes	Yes	Yes	Yes	Yes	Yes	Yes	Yes	Yes	Yes	Yes	Yes	Yes

Table 8
Comparison of cumulative percent change in filtrate loss with respect to time for a 2 mm fracture of drilling muds (Time = 7 min; T = 250 °F; P = 500 psi).

	Nutshell mud system								RH-SNP mud system							
	0.50	1.0	2.0	3.0	4.0	5.0	6.0	7.0	0.50	1.0	2.0	3.0	4.0	5.0	6.0	7.0
% Change in filtrate loss	−20	65	64	82	62	58	58	58	−10	70	87	71	73	73	73	73
Enhancement	No	Yes	Yes	Yes	Yes	Yes	Yes	Yes	No	Yes	Yes	Yes	Yes	Yes	Yes	Yes

resulting in fluid loss (Jeennakorn et al., 2017).

A percent change in filtrate loss with respect to time with 1 mm and 2 mm fracture is presented in Tables 7 and 8, respectively. WBM was used as the control mud to check for a possible enhancement with nutshell and RH-SNP. Briefly, the enhancement in the sealing property of the base mud by both the nutshell and RH-SNP is evident and exceedingly large, as shown in Tables 7 and 8 The enhancement is greater with RH-SNP compared to nutshell. For instance, at a sealing time of 7 min, RH-SNP improved the sealing integrity of the base mud by 87%, while nutshell registered 77% enhancement for a 1 mm fracture (Table 7). Similarly, with a 2 mm fracture at the same time, the sealing integrity of the base mud was enhanced by 58% and 73% by nutshell and RH-SNP, respectfully (Table 8). Further, it was found that the RH-SNP enhancement in combating filtrate loss into the fractured formation is superior to that of the nutshell. Another observation made is the higher sealing performance of the nutshell and RH-SNP in a 1 mm fracture compared to 2 mm fracture; possiibly because it took a longer time for the LCMs (nutshell and RH-SNP) to occupy the void spaces of the formation since the 2 mm fracture is larger than that of 1 mm.

5. Conclusions

This study examined the impact of using environmentally friendly and cost-effective RH-SNP from RH wastes as a fluid loss and lost circulation control agent in complex WBMs. The rheological and filtrate loss control properties of the spud mud with RH-SNP was investigated at a temperature of 80 °F only to understand the effect of the RH-SNP in a spud mud. Thereafter, complex WBM systems were formulated with different concentrations (0.5 wt%, 1.0 wt%, 1.5 wt%, and 2.0 wt%) of RH-SNPs to examine their sealing integrity through bridging material test in a simulated 1 mm and 2 mm fractures to mimic the production zone. Also investigated are the effects of RH-SNP on the rheological and filtration loss control properties of WBM at temperatures of 80 °F and 250 °F. The performance of RH-SNP as a lost circulation agent in complex WBM was investigated and compared with widely applied nutshell used in the petroleum industry. Based on the objectives and results of this study, the following conclusions are presented:

(1) The wet-milling technique was effective in producing RH-SNP of size between 43.9 nm and 59.5 nm through the mechanism of nucleation, growth, capillary effect, Brownian motion, and coalescence.
(2) Results from complex drilling muds at 80 °F revealed that RH-SNP enhanced the rheological properties of the complex WBM of PV = 7 cP. With 0.5, 1.0, 1.5, and 2.0 wt% of RH-SNP, the PV of the WBM increased to 19, 24, 31, and 34 cP, respectively; corresponding to an increment of 171.4%, 242.9%, 342.9%, and 385.8%, which is beneficial for fluid motion and effective hole cleaning.
(3) With amounts of 0.5, 1.0, 1.5, and 2.0 wt%, the RH-SNP minimized the filtrate loss of the base mud of 19 ml to 15, 14, 12, and 10 ml by 21%, 26%, 37%, and 47% at 80 °F, respectively. At 250 °F, the filtrate loss of the base mud remains constant at 19 ml but reduced with 0.5, 1.0, 1.5, and 2.0 wt% RH-SNP to 16, 14, 12, and 11 ml by 16%, 26%, 37%, and 42%, respectively; advantageous for pore sealing and mitigation of lost circulation.
(4) With the use of 1 mm and 2 mm simulated fracture for 7 min, the mud loss volume of the base mud reduced by 50%, 66.7%, 86%, and 90% (for 1 mm) and 40%, 65.7%, 77.1%, and 80% (for 2 mm) with the inclusion of 0.5 wt%, 1.0 wt%, 1.5 wt%, and 2.0 wt% of RH-SNP.
(5) The bridging material test result shows that RH-SNP performed better than the nutshell. The RH-SNP was able to enhance the seal integrity and was more resistant to deformation.
(6) At a sealing time of 7 min with 1 mm fracture, RH-SNP enhanced the seal integrity of the complex WBM by 87%, while nutshell registered 77% enhancement. Likewise, with 2 mm fracture, the sealing potential of the complex WBM is enhanced by 73% and 58% using RH-SNP and nutshell, respectively.
(7) The negative implication of the developed RH-SNP is the production of environmental pollution by particulate emission as a result of direct combustion of the RH. Also, the extraction of SiO_2 directly from RH is not cost-effective or economical given to its large amount. For economic benefit, RH must be utilized first as a fuel for boilers, where it yields RHA as waste before extracting SiO_2 from it.
(8) Nevertheless, the positive implication is the ability of the small size and narrow size distribution of the particles (43.9–59.5 nm) to demonstrate deformation tendency that hindered agglomeration. This supports the strength of the particles to act as viscosifier and stabilizing agent.
(9) Therefore, the use of agro by-product, low-cost raw material, and low extraction costs make RH-SNP and the extraction process a suitable alternative to commercial SiO_2 NP.

Declaration of competing interest

The authors declare no conflict of interest.

Acknowledgement

Radzuan Junin and Mohd Zaidi Jaafar are grateful to Ministry of Higher Education, Malaysia and UTM for the grants used to support this research (Q.J130000.3551.07G12; R.J130000.7851.5F030; Q.J1300003551.06G68; R.J1300007351.4B545)

Nomenclature

API FL	API fluid loss
API	American petroleum institute
AV	Apparent viscosity
$CaCl_2$	Calcium chloride
DW	Deionized water
GS	Gel strength
HPHT FL	High pressure and high temperature fluid loss
HPHT	High pressure and high temperature
LCM	Loss circulation material
Na_2CO_3	Soda ash
NaOH	Caustic soda
NPs	Nanoparticles
PAC	Polyanionic cellulose
PV	Plastic viscosity
RH	Rice husk
RHA	Rice husk ash
RH-SiO_2 NP	Rice husk silica nanoparticle
RH-SNP	Rice husk nanosilica
SiO_2 NP/SNP	Silica nanoparticle
WBM	Water-based mud
YP	Yield point

References

Agi, A., Junin, R., Abbas, A., Gbadamosi, A.O., Azli, N.B., 2019a. Influence of ultrasonic on the flow behavior and disperse phase of cellulose nano-particles at fluid-fluid interface. Nat. Resour. Res. https://doi.org/10.1007/s11053-019-09514-4.

Agi, A., Junin, R., Gbadamosi, A., Abbas, A., Azli, N.B., Oseh, J., 2019b. Influence of nanoprecipitation on crystalline starch nanoparticle formed by ultrasonic assisted weak-acid hydrolysis of cassava starch and the rheology of their solutions. Chem. Eng. Process. Process Intensif. 142, 107556.

Agi, A., Junin, R., Jaafar, M.Z., Mohsin, A., Arsad, A., Gbadamosi, A., Fung, C.K., Gbonhinbor, J., 2020. Synthesis and application of rice husk silica nanoparticles for chemical enhanced oil recovery. J. Mater. Res. Technol. 9 (6), 13054–13066.

Ahasan, M.H., Alvi, M.A., Ahmed, N., Alam, M.S., 2022. An investigation of the effects of synthesized zinc oxide nanoparticles on the properties of water-based drilling fluid. Petrol. Res. 7 (1), 131–137.

Ali, J.A., Kalhury, A.M., Sabir, A.N., Ahmed, R.N., Ali, N.H., Abdullah, A.D., 2020. A state-of-the-art review of the application of nanotechnology in the oil and gas industry with a focus on drilling engineering. J. Pet. Sci. Eng. 191, 107118.

Alsaba, M., Nygaard, R., Saasen, A., Nes, O., 2014. Lost circulation materials capability of sealing wide fractures. In: SPE Deepwater Drilling and Completions Conference. Galveston. https://doi.org/10.2118/17028 5-MS.

Alwated, B., El-Amin, M.F., 2021. Enhanced oil recovery by nanoparticles flooding: from numerical modeling improvement to machine learning prediction. Adv. Geo-Energy Res. 5 (3), 297–317.

Anawe, P.A.L., Efeovbokhan, V.E., Adebayo, T.A., Nwaogwugwu, M., 2004. The effect of rice husk and saw dust on the properties of oil-based mud at varied temperatures. J. Energy Technol. Pol. 41 (11), 11–12.

API RP 13B-1, 2017. API Standard Practice for Field Testing Water–Based Drilling Fluids, fifth ed. API, USA, pp. 1–121.

Blkoor, S.O., Ismail, I., Oseh, J.O., Selleyitoreea, S., Mohd Norddin, M.N.A., Agi, A., Gbadamosi, A.O., 2021. Influence of polypropylene beads and sodium carbonate treated nanosilica in water-based muds for cuttings transport. J. Pet. Sci. Eng. 200, 108435.

Blkoor, S.O., Mohd Norddin, M.N.A., Ismail, I., Oseh, J.O., Agi, A., Gbadamosi, A.O., Okoli, N.O., Onyejekwe, I.M., Risal, A.R., 2022. Amphipathic anionic surfactant modified hydrophilic polyethylene glycol-nanosilica composite as effective viscosifier and filtration control agent for water-based drilling muds. Arab. J. Chem. 15 (4), 103741.

Bao, D., Qiu, Z., Zhao, X., Zhong, H., Chen, J., Liu, J., 2019. Experimental investigation of sealing ability of loss circulation material using the test apparatus with long fracture slot. J. Pet. Sci. Eng. 183, 1063996.

Boyou, N., Ismail, I., Wan Sulaiman, W.R., Haddad, A., Husein, N., Hui, H., Nadaraja, K., 2019. Experimental investigation of hole cleaning in directional drilling by using nano-enhanced water-based drilling fluids. J. Pet. Sci. Eng. 176, 20–231.

Broni-Bediako, E., Amorin, R., 2019. Experimental study on the effects of cement contamination in a water-based mud. Adv. Geo-Energy Res. 3 (3), 314–319.

Chen, H., Wang, W., Martin, J.C., Oliphant, A.J., Doerr, P.A., Xu, J.F., DeBorn, K.M., Chen, C., Sun, L., 2013. Extraction of lignocellulose and synthesis of porous silica nanoparticles from rice husks: a comprehensive utilization of rice husk biomass. ACS Sustain. Chem. Eng. 1, 254–259.

Davarpanah, A., 2018. Integrated feasibility analysis of shale inhibition property by utilization of pore pressure transmission equipment. Petrol. Res. 3 (2), 152–158.

Elochukwu, H., Gholami, R., Dol, S.S., 2017. An approach to improve the cuttings carrying capacity of nanosilica based muds. J. Pet. Sci. Eng. 152, 210–216.

Fattah, K.A., Lashin, A., 2016. Investigation of mud density and weighting materials effect on drilling fluid filter cake properties and formation damage. J. Afr. Earth Sci. 117, 345–357.

Fadairo, A., Adeyemi, G., Ogunkunle, T., Ling, K., Rasouli, V., Effiong, E., Ayoo, J., 2021. Study the suitability of neem seed oil for formulation of eco-friendly oil-based drilling fluid. Petrol. Res. 6 (3), 283–290.

Fereydouni, M., Sabbaghi, F., Saboori, R., Zeinali, S., 2012. Effect of polyanionic cellulose polymer nanoparticles on rheological properties of drilling mud. Int. J. Nanosci. Nanotechnol. 8 (3), 171–174.

Gbadamosi, A.O., Junin, R., Abdalla, Y., Agi, A., Oseh, J.O., 2019a. Experimental investigation of the effects of silica nanoparticle on hole cleaning efficiency of water-based drilling mud. J. Pet. Sci. Eng. 172, 1226–1234.

Gbadamosi, A., Junin, R., Oseh, J.O., Agi, A., Yekeen, N., Abdalla, Y., Ogiriki, S., Yusuff, A., 2019b. Improving hole cleaning efficiency using nanosilica water-based drilling mud. In: SPE Annual International Conference and Exhibition, Lagos, Nigeria.

Ghalambor, A., Salehi, S., Shahri, M.P., 2014. Integrated workflow for lost circulation prediction. In: SPE International Symposium and Exhibition on Formation Damage Control. https://doi.org/10.2118/168123-MS. Lafayette.

Ghosn, R., Mihelic, F., Hochepied, J.F., Dalmazzone, D., 2017. Silica nanoparticles for the stabilization of W/O emulsions at HTHP conditions for unconventional reserves drilling operations. Oil. Gas Sci. Technol. Revue d'IFB Energ. Nouvelles 72 (4), 21–35.

Hamad, B.A., He, M., Xu, M., Liu, W., Mpelwa, M., Tang, S., Jin, L., Song, J., 2020. A novel amphoteric polymer as a rheology-enhancer and fluid-loss control agent for water-based drilling muds at elevated temperatures. ACS Omega 5 (15), 8483–8495.

Ismail, A.R., Mohd, M.N.A.M., Basir, N.F., Oseh, J.O., Ismail, I., Blkoor, S.O., 2020. Improvement of rheological and filtration characteristics of water-based drilling fluids using naturally derived henna leaf and hibiscus leaf extracts. J. Pet. Explor. Prod. Technol. 10, 3541–3556.

Ismail, A.R., Wan Sulaiman, W., Jafaar, M., Ismail, I., Hera, E., 2016. Nanoparticles performance as fluid loss additives in water base drilling fluid. Mater. Sci. Forum 864, 189–193.

Jeennakorn, M., Alsaba, M., Nygaard, R., Saasen, A., Nes, O., 2019. The effect of testing conditions on the performance of lost circulation materials: understandable sealing mechanism. J. Pet. Explor. Prod. Technol. 9, 823–836.

Jeennakorn, M., Nygaard, R., Nes, O., Saasen, A., 2017. Testing conditions makes a difference when testing LCM. J. Nat. Gas Sci. Eng. 46, 375–386.

Khalifeh, M., Klungtvedt, K.R., Vasshus, J.K., Saasen, A., 2019. Drilling fluids-lost circulation treatment. In: SPE Norway One Day Seminar, Bergen, Norway. https://doi.org/10.2118/195609-MS.

Kumar, A., Savari, S., 2011. Lost circulation control and wellbore strengthening: looking beyond particle size distribution. In: AADE National Technical Conference and Exhibition (Houston).

Kumar, S., Sidek, M.A., Agi, A., Junin, R., Jaafar, M.Z., Gbadamosi, A., Gbonhinbor, J., Oseh, J.O., Yakasai, F., 2021. Decommissioning of offshore oil and gas facilities: a comparative study between Malaysia practices and international standards. In: SPE Nigeria Annual International Conference and Exhibition, Lagos, Nigeria.

Lecolier, E., Herzhaft, B., Rousseau, L., Neau, L., 2005. Development of a nanocomposite gel for lost circulation treatment. In: SPE Formation Damage Conference. Scheveningen, Netherlands.

Lohrasb, S., Junin, R., Agi, A., Jaafar, M.Z., Gbadamosi, A., Sidek, M.A., Gbonhinbor, J., Oseh, J.O., 2021. Analytical model for estimation of pore volume to breakthrough in carbonate acidizing with organic and mineral acids. In: SPE Nigeria Annual International Conference and Exhibition, Lagos, Nigeria.

Mahto, V., Jain, R., 2013. Effect of fly ash on the rheological and filtration properties of water based drilling fluids. Int. J. Renew. Energy Technol. 2 (8), 50–156.

Medhi, S., Chowdhury, S., Gupta, D.K., Mazumdar, A., 2020. An investigation on the effects of silica and copper oxide nanoparticles on rheological and fluid loss property of drilling fluids. J. Pet. Explor. Prod. Technol. 10, 91–100.

Ngouangna, E.N., Manan, M.A., Oseh, J.O., Norrdin, M.N.A.M., Agi, A., Gbadamosi, A.O., 2020. Influence of (3–Aminopropyl) triethoxysilane on silica nanoparticle for enhanced oil recovery. J. Mol. Liq. 315, 113740.

Okon, A.N., Udoh, F.D., Bassey, P.G., 2014. Evaluation of rice husk as fluid loss control additive in water-based drilling mud. In: SPE Nigeria Annual International Conference and Exhibition, Lagos, Nigeria.

Oseh, J.O., Norddin, M.N.A., Ismail, I., Gbadamosi, A.O., Agi, A., Muhammed, H.N., 2019a. A novel approach to enhance rheological and filtration properties of water–based mud using polypropylene–silica nanocomposite. J. Pet. Sci. Eng. 181, 106264.

Oseh, J.O., Norrdin, M.N.A.M., Farooqi, F., Ismail, A.R., Ismail, I., Gbadamosi, A.O., Agi, A., 2019b. Experimental investigation of the effect of henna leaf extracts on cuttings transportation in highly deviated and horizontal wells. J. Pet. Explor.

Prod. Technol. 9, 2387–2404.
Oseh, J.O., Norddin, M.N.A., Ismail, I., Ismail, A.R., Gbadamosi, A.O., Agi, A., 2020a. Effect of the surface charge of entrapped polypropylene at nanosilica-composite on cuttings transport capacity of water-based muds. Appl. Nanosci. 10, 61–82.
Oseh, J.O., Norddin, M.N.A., Ismail, I., Gbadamosi, A.O., Agi, A., Ismail, A.R., 2020b. Experimental investigation of cuttings transportation in deviated and horizontal wellbores using polypropylene–nanosilica composite drilling mud. J. Pet. Sci. Eng. 189, 106958.
Oseh, J.O., Norddin, M.N.A., Ismail, I., Gbadamosi, A.O., Agiv, A., Ismail, A.R., 2020c. Study of cuttings lifting with different annular velocities using partially hydrolyzed polyacrylamide and enriched polypropylene–nanosilica composite in deviated and horizontal wells. Appl. Nanosci. 10, 971–993.
Oseh, J.O., Norddin, M.N.A., Muhammed, H.N., Ismail, I., Gbadamosi, A.O., Agi, A., Ismail, A.R., Blkoor, S.O., 2020d. Influence of (3–Aminopropyl) triethoxysilane on entrapped polypropylene at nanosilica composite for shale swelling and hydration inhibition. J. Pet. Sci. Eng. 194, 1–16.
Panchal, H., Patel, H., Patel, J., Shah, M., 2021. A systematic review on nanotechnology in enhanced oil recovery. Petrol. Res. 6 (3), 204–212.
Rafati, R., Smith, S.R., Haddad, A.S., Novara, R., Hamidi, H., 2018. Effect of nanoparticles on the modifications of drilling fluids properties: a review of recent advances. J. Petrol. Sci. Eng. 161, 61–76.
Rajesh, K.M., Ajitha, B., Ashok, K.R.Y., Suneetha, Y., Sreedhara, R.P., 2016. Synthesis of copper nanoparticles and role of pH on particle size control. Mater. Today Proc. 3, 1985–1991.
Saleh, T.A., 2022. Advanced trends of shale inhibitors for enhanced properties of water-based drilling fluid. Upstream Oil Gas Technol. 8, 100069.
Saleh, T.A., AL-Hammadi, S.A., 2018. Insights into the fundamentals and principles of the oil and gas industry: the impact of nanotechnology. In: Saleh, T. (Ed.), Nanotechnology in Oil and Gas Industries. Springer, Cham. https://doi.org/10.1007/978-3-319-60630-9_1.
Saleh, T.A., Ibrahim, M.A., 2021. Synthesis of amyl ester grafted on carbon-nanopolymer composite as an inhibitor for cleaner shale drilling. Petroleum. https://doi.org/10.1016/j.petlm.2021.07.002.
Salehi, S., Nygaard, R., 2012. Numerical modeling of induced fracture propagation: a novel approach for lost circulation materials (LCM) design in borehole strengthening applications of deep offshore drilling. In: SPE Annual Technical Conference and Exhibition (San Antonio).
Singh, R., Dutta, S., 2018. Synthesis and characterization of solar photoactive TiO_2 nanoparticles with enhanced structural and optical properties. Adv. Powder Technol. 9 (2), 211–219.
Smith, S.R., Rafati, R., Haddad, A.S., Cooper, A., Hamidi, H., 2018. Application of aluminium oxide nanoparticles to enhance rheological and filtration properties of water-based mud at HPHT conditions. Colloids Surf. A Physicochem. Eng. Asp. 537, 361–371.
Wang, W., Martin, J.C., Fan, X., Han, A., Luo, Z., Sun, L., 2012. Silica nanoparticles and frameworks from rice husk biomass. ACS Appl. Mater. Interfaces 4 (2), 977–981.
Xuan, Y., Jiang, G., Li, Y., 2014. Nanographite oxide as ultra strong fluid-loss-control additive in water-based drilling fluids. J. Dispersion Sci. Technol. 35, 1386–1392.
Yildirim, M., Sumnu, G., Sahin, S., 2016. Rheology, particle-size distribution, and stability of low-fat mayonnaise produced via double emulsion. Food Sci. Biotechnol. 25, 1613–1618.
Zhang, Z., Cui, J., Wang, B., Wang, Z., Kang, R., Guo, D., 2017. A novel approach of mechanical chemical grinding. J. Alloys Compd. 726, 514–524.
Zhang, Z., Zhang, X., Xu, X., Guo, D., 2013. Characterization of nanoscale chips and a novel model for face nanogrinding on soft brittle HgCdTe films. Tribol. Lett. 49, 203–215.